SOILS AND FOUNDATIONS Vol. 32, No. 2, 125-133, June 1992
Japanese Society of Soil Mechanics and Foundation Engineering

APPLICATION HEIGHT CONTROL SYSTEM OF A BULLDOZER TOWING A SCRAPER DOWN A WEAK SLOPE TERRAIN DURING BRAKING ACTION

TATSURO MURO[i)]

ABSTRACT

On earth moving sites, it is considered very important for the application height of effective braking force of a bulldozer towing a scraper down a weak slope terrain to be controlled in accordance with the pushing force of the scraper in order to avoid excessive wear of the track belt. Here, the tracking performance of a flexible tracked vehicle towing a scraper down at a constant speed on a given remolded silty loam sloping terrain is analysed by the use of a simulation program. As a result, it is clarified that the optimum application height under the maximum braking power decreases with the increment of pushing force of the scraper, and that the height should be controlled automatically according to the pushing force of the scraper, which is dependent on the slope angle.

Key words: application height, effective braking force, flexible tracked vehicle, slope, weak terrain (**IGC**: K4/K5)

INTRODUCTION

When a bulldozer is towing a scraper while transportation earth down a weak slope terrain at an earthmoving site during highway construction, the bulldozer can be operated during braking action at a constant speed, and the application height (Yong et al., 1984) of the effective braking force should be controlled to the optimum height at the slip ratio, developing the maximum braking power in accordance with the pushing force of the scraper, in order to avoid excessive wear of the track belt.

For the given vehicle dimensions and the terrain-track system constants, the force and energy balance equations for the bulldozer towing a scraper down a weak slope terrain are developed. Then, several tracking performance characteristics of the flexible tracked vehicle moving down at a constant speed on a given remolded silty loam sloping terrain are simulated precisely by the use of a simulation program which predicts the method of determination of the optimum effective braking force from the drag force developed on the interface between the track belt and the terrain, and from the locomotion resistance, etc. This paper also clarifies the relations between various performance factors (including brak-

[i)] Prof. Department of Civil and Ocean Engineering, Faculty of Engineering, Ehime University, 3 Bunkyo-cho, Matsuyama 790.
Manuscript was received for review on March 1, 1991.
Written discussions on this paper should be submitted before January 1, 1993, to the Japanese Society of Soil Mechanics and Foundation Engineering, Sugayama Bldg. 4F, Kanda Awaji-cho 2-23, Chiyoda-ku, Tokyo 101, Japan. Upon request the closing date may be extended one month.

ing force, effective braking force, sinkages, eccentricity of resultant normal force, trim angle, energies, braking efficiency of power) and slip ratio, and the relations between the contact pressure distribution under track belt and slip ratio. Next, the automated control system which controls the optimum application height of the effective braking force is considered in accordance with the pushing force of the scraper.

TERRAIN-VEHICLE SYSTEM

The terrain-track system constants (Muro et al., 1990) measured for a track model having 5 equilateral trapezoid grousers of height $H=6.0$ cm, and pitch $G_p=18.0$ cm, of which the upper length is 2.0 cm and the lower length is 8.9 cm, are shown in Table 1. The terrain is composed of remolded weak silty loam of 30% water content and 31 kPa Cone Index.

For the track plate loading test:

$$p \leqq p_0: \quad p=k_1 s_0^{n1} \tag{1}$$

$$p > p_0: \quad p=p_0+k_2(s_0-H)^{n2} \tag{2}$$

$$p_0=k_1 H^{n1}$$

For the track plate traction test:

$$\tau=(m_c+m_f p)\{1-\exp(-aj)\} \tag{3}$$

For the track plate slip sinkage test:

$$s_s=c_0 p^{c1} j^{c2} \tag{4}$$

where p (kPa) is the contact pressure, s_0 (cm) and s_s (cm) are the amounts of static and slip sinkage, and j (cm) is the amount of slippage.

Table 1. Terrain-track system constants

Track plate loading test	
$p \leqq p_0$	$k_1=2.255$
	$n_1=1.120$
$p > p_0$	$k_2=6.669$
	$n_2=5.938\times10^{-1}$
Track plate traction test	
	$m_c=3.626$ kPa
	$m_f=0.356$
	$a=0.148$ 1/cm
Track plate slip sinkage test	
	$c_0=0.253$
	$c_1=0.751$
	$c_2=0.360$

The vehicle dimensions of a given bulldozer are as follows: vehicle weight $W=150$ kN, width of track belt $B=150$ cm, contact length of track belt $D=320$ cm, mean contact pressure $p_m=15.6$ kPa, radius of front idler and rear sprocket $R_f=R_r=35$ cm, interval of track roller $R_p=40$ cm, eccentricity of gravity center of vehicle $e=-0.05\sim0.05$, height of gravity center $h_g=70$ cm, distance between central axis of vehicle and application point of effective braking force $l_d=310$ cm, height of application point of effective braking force $h_d=-140$ cm ~ 140 cm. The flexible track belt is made up of the same track model plate and grousers as mentioned previously, and the initial track tension force H_0 is given as 9.8 and 49.0 kN.

FORCE AND ENERGY BALANCE ON A SLOPE

Fig. 1 shows the dimensions and the various forces acting on a bulldozer trailing a scraper down a weak slope terrain. The negative braking torque Q is applied to the sprocket and the negative braking force T_1 pulls the upper part of the track belt. The compaction resistance T_2 acts in parallel with the terrain surface of the slope angle β on the front part of the track belt at depth z_i. Assuming that the track belt is freely rolling, the depth z_i is determined as follows:

$$z_i=s'_{ri}-\left[T_2\left\{R_r+(h_d-R_r)\cos\theta'_{ti}-\left(l_d-\frac{D}{2}\right)\sin\theta'_{ti}\right\}-W\left\{h_g\sin(\theta'_{ti}+\beta)-D\left(\frac{1}{2}-e\right)\cos(\theta'_{ti}+\beta)\right\}\right]\Bigg/\left\{T_2+\frac{W\cos(\beta+\theta'_{ti})}{\tan\theta'_{ti}}\right\} \tag{5}$$

where s'_{ri} is the amount of sinkage of the rear sprocket and θ'_{ti} is the trim angle of the vehicle. The negative drag T_3 acts along the grouser tips of the bottom track belt. The negative effective braking force T_4 acts in parallel with the terrain surface.

The slip ratio i_b during braking action is

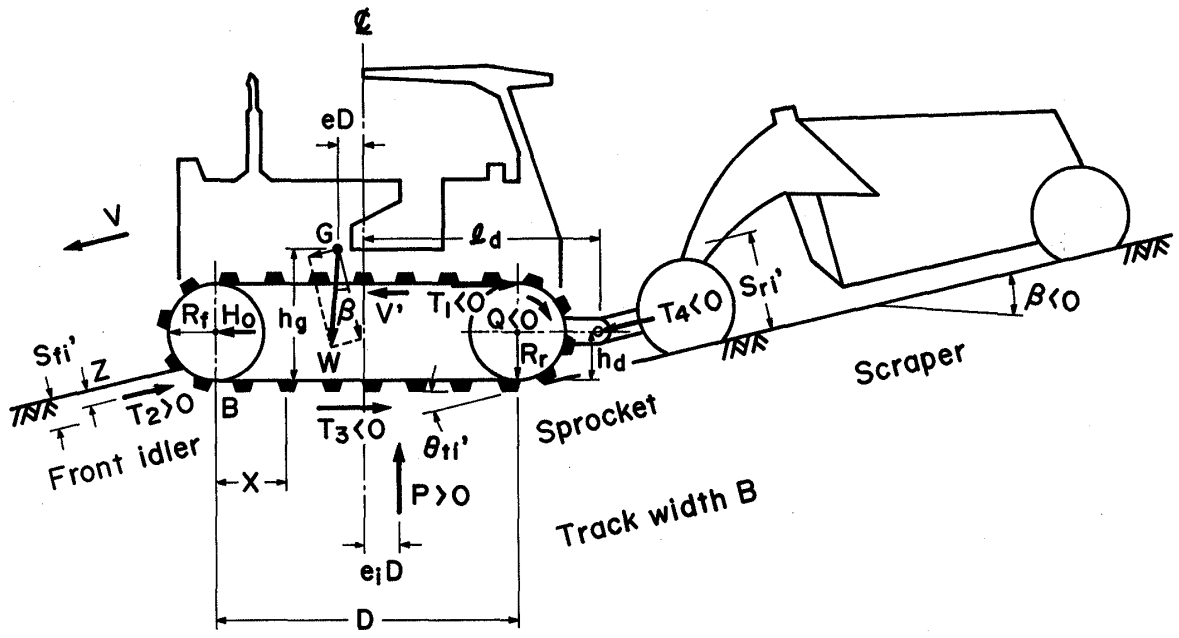

Fig. 1. Various forces acting on a bulldozer towing a scraper down a weak slope terrain

given by the vehicle speed V along the terrain surface and the rotation speed of the track belt V' at the periphery of the rear sprocket as

$$i_b=\frac{V'}{V}-1. \tag{6}$$

As the external braking torque T_3R_r equals the internal torque $Q=T_1R_r$, the eccentricity e_i of the resultant normal force P can be calculated from the balance of moment around the rear wheel axis as

$$e_i=\frac{1}{2}+\frac{1}{PD}\left[-T_2(R_r-s_{ri}'+z_i)+T_4\left\{(h_d-R_r)\cos\theta_{ti}'-\left(l_d-\frac{D}{2}\right)\sin\theta_{ti}'\right\}+W\left\{(h_g-R_r)\sin(\theta_{ti}'+\beta)-D\left(\frac{1}{2}-e\right)\times\cos(\theta_{ti}'+\beta)\right\}\right]. \tag{7}$$

The force balances between T_2, T_3, T_4, P and W are given for both directions, parallel and normal to the terrain surface, as

$$T_2+T_4=T_3\cos\theta_{ti}'-P\sin\theta_{ti}'-W\sin\beta \tag{8}$$

and

$$W\cos\beta=P\cos\theta_{ti}'+T_3\sin\theta_{ti}'. \tag{9}$$

Then the value

$$T_4=\frac{T_3}{\cos\theta_{ti}'}-W\cdot\frac{\sin(\beta+\theta_{ti}')}{\cos\theta_{ti}'}-T_2 \tag{10}$$

is determined.

The effective input energy E_1 supplied by the braking torque is the sum of the output energies, which are: (a) the sinkage deformation energy E_2 required to make a rut under the track belt, (b) the slippage energy E_3 developed at the bottom track belt, (c) the effective braking force energy E_4, and (d) the variation of potential energy E_5.

$$E_1=E_2+E_3+E_4+E_5 \tag{11}$$

If these energy values are calculated as the unit energy per second, each relation between energy and force is given by

$$E_1=T_3V(1+i_b) \tag{12}$$

$$E_2=T_2V \tag{13}$$

$$E_3=T_3\left\{(1+i_b)-\frac{1}{\cos\theta_{ti}'}\right\}V+WV\tan\theta_{ti}'\cos\beta \tag{14}$$

$$E_4=T_4V \tag{15}$$

$$E_5=WV\sin\beta \tag{16}$$

and the braking efficiency of power E_b is given

as the ratio of effective braking power to input power as

$$E_b=\frac{VT_4}{V'T_1}=\frac{T_4}{(1+i_b)T_1}. \tag{17}$$

TRACKING PERFORMANCE DURING BRAKING ACTION

Drag Force

The drag force T_3 can be calculated as the summation of the drag T_{mb}, T_{ms} developed on the main part of the bottom track belt, on the side parts of the grousers, the drag T_{fb}, T_{fs} developed on the contact parts of the front idler, and the drag T_{rb}, T_{rs} developed on the contact parts of the rear sprocket (Muro, 1989). For the flexible track belt, T_{mb} and T_{ms} for the positive static sinkage can be presented as

$$T_{mb}=2B\int_0^{DD}\{m_c+m_f\cdot p_i'(X)\}\cdot\{1-\exp(-a\cdot j_m)\}\,dX$$
$$-2B\int_{DD}^{D}\{m_c+m_f\cdot p_i'(X)\}\cdot\{1-\exp(a\cdot j_m)\}\,dX \tag{18}$$

$$T_{ms}=4H\int_0^{DD}\left\{m_c+m_f\frac{p_i'(X)}{\pi}\cot^{-1}\left(\frac{H}{B}\right)\right\}\{1-\exp(-a\cdot j_m)\}\,dX$$
$$-4H\int_{DD}^{D}\left\{m_c+m_f\frac{p_i'(X)}{\pi}\cot^{-1}\left(\frac{H}{B}\right)\right\}\{1-\exp(a\cdot j_m)\}\,dX \tag{19}$$

$$j_m=\frac{(1+i_b)-\cos\theta_{ti}'}{1+i_b}X+j_B$$

$$DD=-j_B\cdot\frac{1+i_b}{(1+i_b)-\cos\theta_{ti}'}$$

$$p_i'(X)=k_1\{s_{0i}'(X)\}^{n1}\quad\text{for}\quad 0\leqq s_{0i}'(X)\leqq H$$

$$p_i'(X)=p_0+k_2\{s_{0i}'(X)-H\}^{n2}\quad\text{for}\quad s_{0i}'(X)>H$$

where j_B is the amount of slippage at point B and $s_{oi}'(X)$ is the amount of static sinkage of the flexible track belt (Muro, 1990a) at the distance X from point B.

The track tension T_0 is given as the summation of initial track tension force H_0 and drag force H_m acting on the interface between the track belt and the terrain. H_m can be calculated as the integration of shear resistance $\tau(X)$ of the terrain from $X=D$ to $X=D-(20m-10)d$ as

$$H_m=-\int_D^{D-(20m-10)d}\tau(X)\,dX \tag{20}$$

where $d=D/160$ and $m=1, 2, \cdots, 8$ (the number of road roller intervals on the track belt).

Compaction Resistance

The main locomotion resistance against the bulldozer is the compaction resistance T_2 required to make ruts under the track belt due to the static and slip sinkage. T_2 can be calculated from the sinkage deformation energy E_2' during the running distance of the bulldozer for the moving distance D of the track belt as

$$E_2'=\frac{D\cos\theta_{ti}'}{1+i_b}\left(1+\frac{H}{R_r}\right)\cdot T_2$$
$$=\frac{2BD\cos\theta_{ti}'}{1+i_b}\left(1+\frac{H}{R_r}\right)\int_0^{s_{ri}'}p\,ds \tag{21}$$

and for $s_{ri}'\geqq H$

$$T_2=2B\left[\int_0^{H}k_1s^{n1}\,ds+\int_H^{s_{ri}'}\{p_0+k_2(s-H)^{n2}\}\,ds\right]$$
$$=\frac{2k_1B}{n_1+1}H^{n_1+1}+2k_1BH^{n1}(s_{ri}'-H)$$

$$+\frac{2k_2B}{n_2+1}(s'_{ri}-H)^{n2+1}. \tag{22}$$

The total amount of sinkage of the rear sprocket s'_{ri} is the summation of the amount of static sinkage s'_{roi} and that of slip sinkage s'_{rsi} which is calculated for the flexible track belt.

$$s'_{ri}=(s'_{roi}+s'_{rsi})\cos\theta'_{ti} \tag{23}$$

where

$$s'_{rsi}=s'_{fsi}+c_0\sum_{n=1}^{N}\{p'_i(nd)\}^{c1}\times\left[\left(\frac{n}{N}j'_D\right)^{c2}-\left(\frac{n-1}{N}j'_D\right)^{c2}\right] \tag{24}$$

$$j'_D=-\left(\frac{1+i_b}{\cos\theta'_{ti}}-1\right)D$$

$$d=D/N$$

$$s'_{fsi}=c_0\sum_{m=1}^{M}\{p_f(\theta_m)\cos\theta_m\}^{c1}\times\left\{\left(\frac{m}{M}j_{fs}\right)^{c2}-\left(\frac{m-1}{M}j_{fs}\right)^{c2}\right\} \tag{25}$$

$$\theta_m=\theta_f\left(1-\frac{m}{M}\right)$$

$$\theta_f=\cos^{-1}\left(\cos\theta'_{toi}-\frac{s'_{foi}}{R_f}\right)-\theta'_{toi}$$

$$\theta'_{toi}=\tan^{-1}\{s'_{roi}-s'_{foi})/D\}$$

$$j_{fs}=-(R_f+H)i_b\sin\theta_f$$

Optimum Effective Braking Force

The simulation program developed previously (Muro, 1990b) can be revised to calculate the tracking performance of a flexible-tracked vehicle towing a scraper down a weak slope terrain during braking action. First, the initial data including the vehicle dimensions, the terrain-track system constants and the slope angle are given. Then, the amount of static sinkage and the non-linear contact pressure distribution are determined assuming a rigid track belt.

Next, the distribution of total sinkage $s'_i(X)$ is determined as the summation of the static sinkage $s'_0(X)$ and the slip sinkage $s'_s(X)$ which are calculated from the contact pressure $p'_i(X)$ for the flexible track belt. Finally, the effective braking force T_4 can be determined from T_2, T_3, W, θ'_{ti} and β, and the relations between T_1, T_4-i_b, s'_{fi}, $s'_{ri}-i_b$, e_i, $\theta'_{ti}-i_b$ and E_1, E_2, E_3, E_4, E_5-i_b and the distributions of normal pressure $p'_i(X)$, and shear resistance $\tau'_i(X)$ are graphically shown by use of microcomputer. The optimum effective braking force T_{4opt} is defined as T_4 for the optimum slip ratio i_{bopt} at which the effective input energy $|E_1|$ reaches the maximum braking power.

ANALYTICAL RESULTS

As an example, the tracking performance of the bulldozer trailing a scraper down a weak slope terrain during braking action has been simulated for e$=-0.02$, $h_d=80$ cm, $H_0=9.8$ kN and $\beta=-0.349$ rad.

Fig. 2 shows the relations between T_1, T_4 and i_b, in which the absolute values $|T_1|$ and $|T_4|$ increase rapidly with the increment of $|i_b|$ at the smaller range and increase gradually at the larger range of slip ratio. $|T_1|$ is always larger than $|T_4|$ due to the increasing locomotion resistance T_2 with $|i_b|$. Fig. 3 shows the relations between s'_{fi}, s'_{ri} and i_b, in which s'_{ri} is always larger than s'_{fi} due to the increasing slip sinkage with $|i_b|$. And s'_{fi}, s'_{ri} increase rapidly with the increment of $|i_b|$ at the smaller range, but increase almost linearly at the larger range. Fig. 4 shows the relations be-

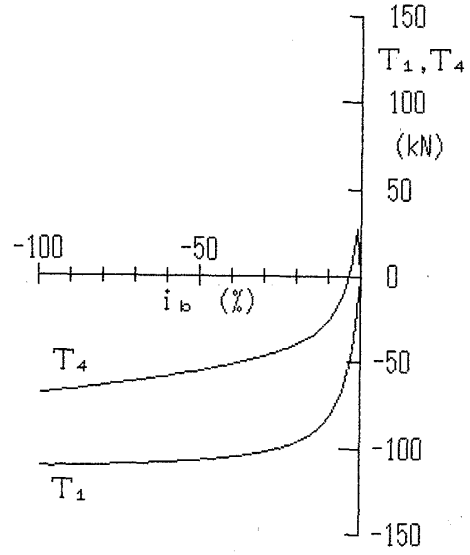

Fig. 2. Relations between braking force T_1, effective braking force T_4 and slip ratio i_b ($\beta=-0.349$ rad)

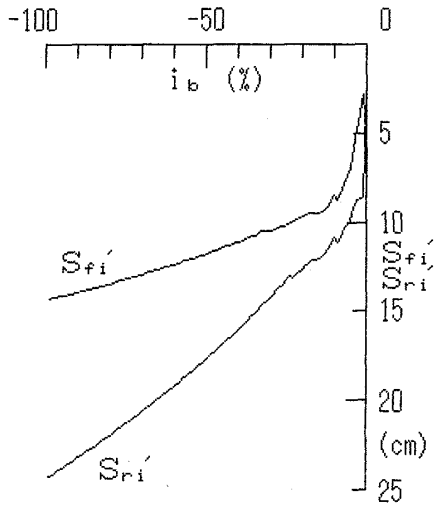

Fig. 3. Relations between amounts of sinkage of front idler s_{fi}', rear sprocket s_{ri}' and slip ratio i_b ($\beta=-0.349$ rad)

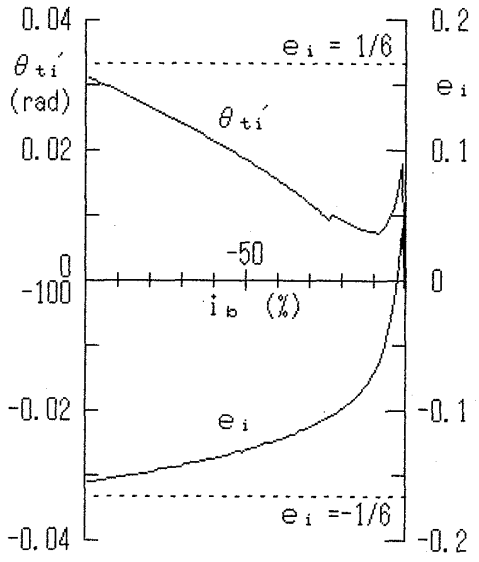

Fig. 4. Relations between trim angle θ_{ti}', eccentricity e_i and slip ratio i_b ($\beta=-0.349$ rad)

tween θ_{ti}', e_i and i_b, in which θ_{ti}' increases almost linearly with the increment of $|i_b|$ from the minimum value 0.00731 rad at $i_b=-9\%$, and e_i decreases parabolically with the increment of $|i_b|$. Fig. 5 shows the relations between E_1, E_2, E_3, E_4, E_5 and i_b for $V=9.4$ cm/s. $|E_1|$ has the maximum value 733.9 kNcm/s at $i_{bopt}=-16\%$. E_2, E_3 increase almost linearly with the increment of $|i_b|$. $|E_4|$ increases parabolically with $|i_b|$, but $|E_5|$ decreases slightly with $|i_b|$ from the maximum value 553.6 kNcm/s at $i_b=-9\%$. In this case, $T_{4opt}=-35.88$ kN and the optimum braking force $T_{1opt}=-92.94$ kN, and the corresponding $s_{ri}'=12.10$ cm, $\theta_{ti}'=0.00819$ rad, $e_i=-0.0917$ and $E_b=46.0\%$.

Fig. 6(a) shows the distributions of normal

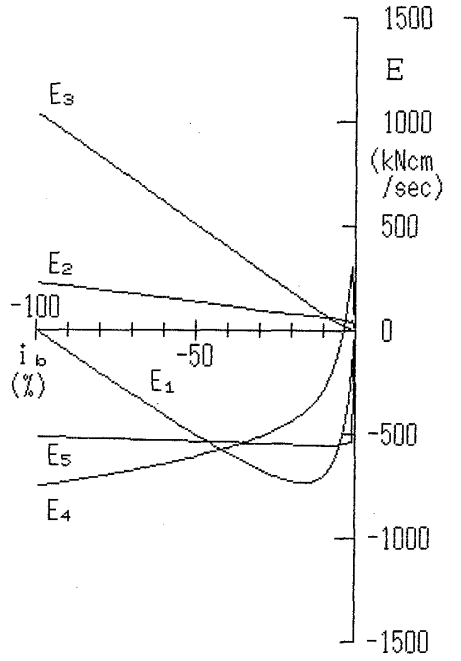

Fig. 5. Relations between energy values E_1, E_2, E_3, E_4, E_5 and slip ratio i_b ($\beta=-0.349$ rad)

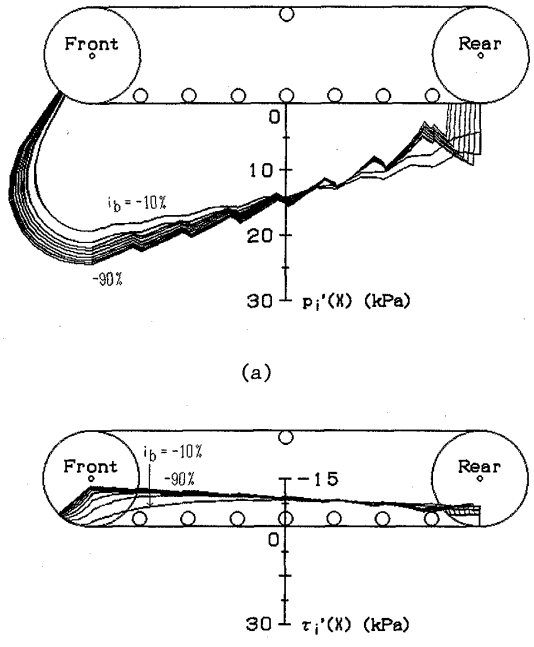

Fig. 6. Distributions of contact pressure during braking action ($H_0=9.8$ kN, $\beta=-0.349$ rad) (a) normal pressure $p_i'(X)$ (b) shear resistance $\tau_i'(X)$

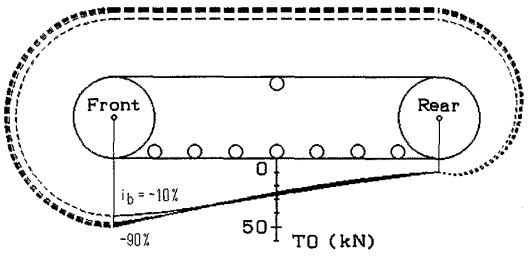

Fig. 7. Distributions of track tension T_0 around the track belt for various slip ratios i_b (H_0=9.8 kN, β=−0.349 rad)

pressure $p_i'(X)$ during braking action for various slip ratios. They show positive values for the entire contact portion of the track belt. For all slip ratios, the distributions decline forward to the contact part of the front idler, and $p_i'(X)$ at point B tends to increase with the increment of $|i_b|$ due to the decreasing eccentricity e_i. Fig. 6(b) shows the distributions of shear resistance $\tau_i'(X)$ under the track belt during braking action for various slip ratios. They show negative values for the entire contact portion of the track belt, but $\tau_i'(X)$ at i_b=−10% changes from a positive value to a negative value at some point on the contact part of the front idler in accordance with the amount of slippage change. Fig. 7 shows the distributions of track tension around the track belt for various slip ratios.

OPTIMUM APPLICATION HEIGHT

Here, the optimum application height of the effective braking force h_{dopt} is defined as the height at which the pushing force of a scraper applied to the bulldozer on a slope terrain agrees well with the optimum effective braking force T_{4opt}.

Several relations between T_{4opt}, s_{ri}', θ_{ti}', e_i, E_b and h_{dopt} have been calculated for the given vehicle dimensions at H_0=49.0 kN, e=−0.05, 0.00, 0.05, h_d=−140 cm to 140 cm in increments of 20 cm and β=−0.349 rad. Figs. 8(a) and (b) show the relations between T_{4opt} and the corresponding optimum braking force T_{1opt} and h_{dopt} for the given eccentricities. For e=−0.05, the larger the values of $|T_{1opt}|$ and $|T_{4opt}|$, the lower the values of h_{dopt}. However, for e=0.00 and +0.05, $|T_{1opt}|$ and

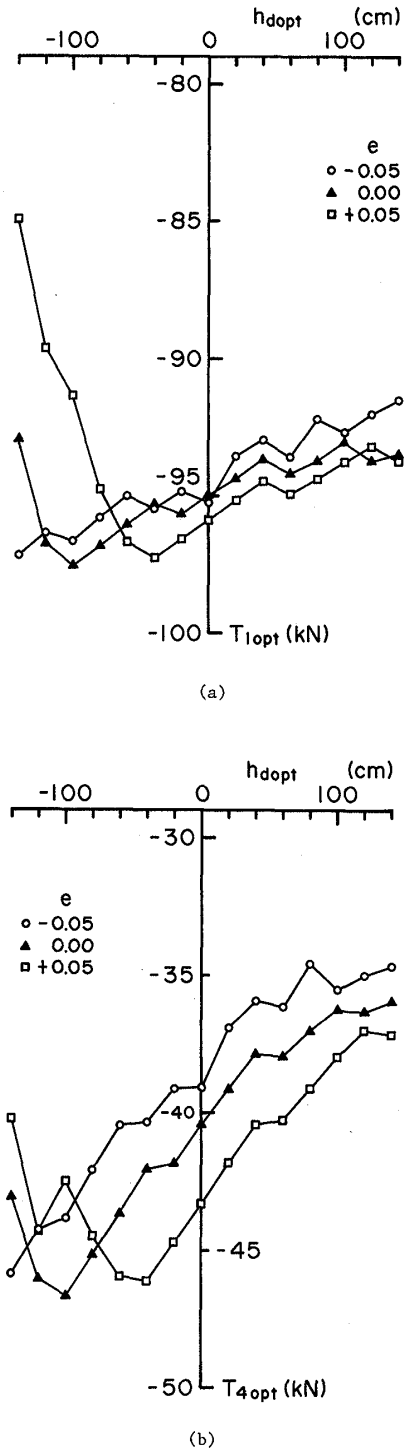

Fig. 8. Relations between optimum braking force T_{1opt}, optimum effective braking force T_{4opt} and optimum application height h_{dopt} (H_0=49.0 kN, β=−0.349 rad) (a) optimum braking force (b) optimum effective braking force

$|T_{4opt}|$ reach the maximum values at h_{dopt}=−100 cm and −40 cm, respectively. In general, the larger the value of e, the larger the values of $|T_{1opt}|$ and $|T_{4opt}|$ which are devel-

oped for the positive value of h_{dopt}. Fig. 9 shows the relations between s'_{ri} and h_{dopt}, in which s'_{ri} takes the minimum value at $h_{dopt}=80$ cm for $e=-0.05$, at $h_{dopt}=80$ cm for $e=0.00$, and at $h_{dopt}=120$ cm for $e=0.05$. In general, s'_{ri} increases gradually with the increment of e_i, as shown later. Fig. 10 shows the relations between θ'_{ti} and h_{dopt}, in which θ'_{ti} decreases hyperbolically with the increment of h_{dopt}. Fig. 11 shows the relations between e_i and h_{dopt}, in which e_i decreases with the increment of h_{dopt} and with the decrement of e. Fig. 12 shows the relations between E_b and h_{dopt}, in which E_b

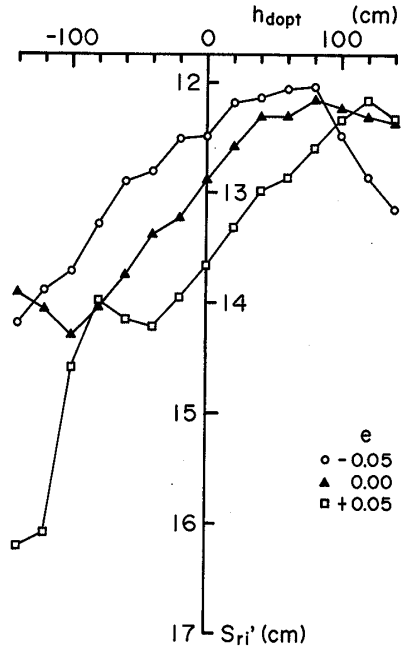

Fig. 9. Relations between amount of sinkage of rear sprocket s'_{ri} and optimum height h_{dopt} ($H_0=49.0$ kN, $\beta=-0.349$ rad)

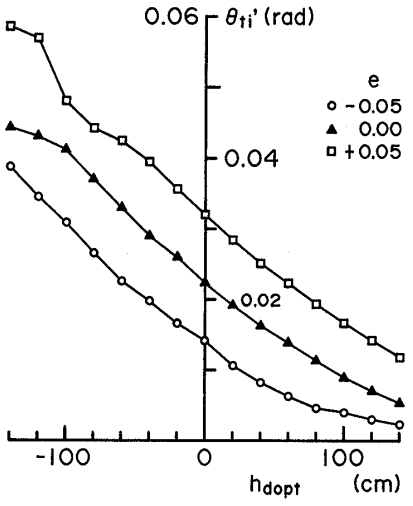

Fig. 10. Relations between trim angle of bulldozer θ'_{ti} and optimum height h_{dopt} ($H_0=49.0$ kN, $\beta=-0.349$ rad)

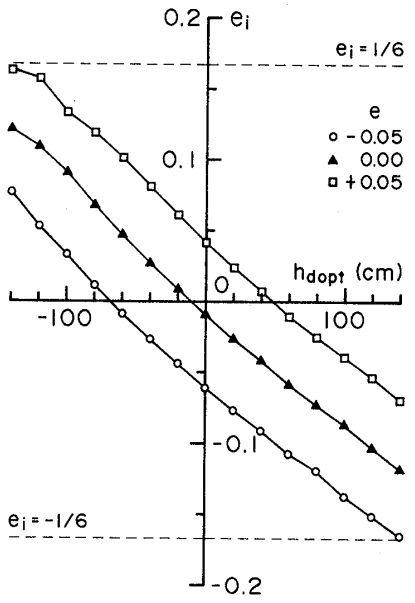

Fig. 11. Relations between eccentricity of resultant normal force e_i and optimum height h_{dopt} ($H_0=49.0$ kN, $\beta=-0.349$ rad)

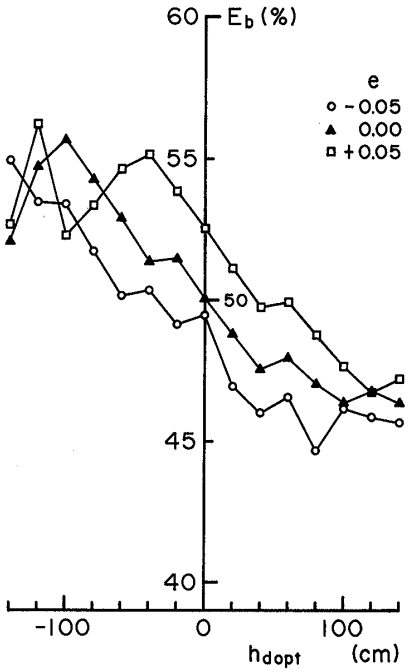

Fig. 12. Relations between braking efficiency of power E_b and optimum height h_{dopt} ($H_0=49.0$ kN, $\beta=-0.349$ rad)

decreases gradually with the increment of h_{dopt} and with the decrement of e, in correspondence with the difference between T_{1opt} and T_{4opt}.

In general, the larger the weight of the scraper (i.e. the pushing force), the larger the braking efficiency of power. For the negative value of h_{dopt}, the pushing force of the scraper becomes the sum of T_{4opt} and the excavating force of the braking shank of the bulldozer.

AUTOMATED CONTROL SYSTEM

To control the optimum application height of effective braking force automatically, the relation between T_{4opt} and h_{dopt} should be determined for the given bulldozer. In this case, the terrain-track system constants used to calculate the relations could be automatically measured for the various combinations of running terrain properties and vehicle dimensions (Muro, 1988). Then the optimum application height h_{dopt} can be immediately decided from T_{4opt}, measured as the pushing force of the scraper by use of some type of load sensor.

Therefore, a new automated control system for control of optimum application height should be developed to control the given height h_{dopt} within ± 10 cm.

CONCLUSIONS

The proposed application height control system for a bulldozer towing a scraper down a weak slope during braking action could be summarized as follows:

(1) The terrain-track system constants should be determined in-situ, by measuring the initial amount of sinkage, and the torques and the amount of slip sinkage for the three slip ratios.

(2) The vehicle dimensions and the slope angle of the terrain should be given together with the terrain-track system constants as the input data of a micro-computer.

(3) The relation between the optimum effective braking force and the optimum application height could be determined by simulating the total tracking performance.

(4) The optimum application height could be determined from the pushing force of the scraper by use of some type of load sensor.

(5) In general, the larger the absolute value of the pushing force of the scraper, the lower the optimum application height; the application height should be controlled so that the greatest braking efficiency of power can be obtained.

REFERENCES

1) Muro, T. (1988): "An optimum operation of a bulldozer running on a weak terrain," Proc. of 5th Int. Sympo. on Robotics in Construction, JSCE, Vol. 2, pp. 717–726.
2) Muro, T. (1989): "Stress and slippage distribution under track belt running on a weak terrain," SOILS AND FOUNDATIONS, Vol. 29, No. 3, pp. 115–126.
3) Muro, T., Kawahara, S. and Nagira, A. (1990): "Influences of points of application on acting forces of bulldozer running on weak terrain," Memoirs of the Faculty of Engineering, Ehime University, Vol. XII, No. 1, pp. 467–478 (in Japanese).
4) Muro, T. (1990a): "Automated tension control system of track belt for bulldozing operation," Proc. of 7th Int. Sympo. on Automation and Robotics in Construction, Vol. 2, pp. 415–422.
5) Muro, T. (1990b): "Control system of the optimum height of application forces for a bulldozer running on weak terrain," Proc. of the First Symposium on Construction Robotics in Japan, JSCE et al., pp. 197–206 (in Japanese).
6) Yong, R. N., Elmamlouk, H. and Skiadas, N. (1984): "Effect of hitch positions on the performance of track/grouser systems", Proc. of 8th Int. Conference of ISTVS, Vol. 1, pp. 381–397.